Effect of CTE and Stiffness Mismatches on Interphase and Particle Fractures of Zirconium Carbide /AA5050 Alloy Particle-Reinforced Composites

A. Chennakesava Reddy

Associate Professor, Department of Mechanical Engineering, Vasavi College of Engineering, Hyderabad, India
dr_acreddy@yahoo.com

Abstract: *In the present work, the AA5050/ZrC metal matrix composites were manufactured at 10% and 30% volume fractions of ZrC. The composites were subjected to mechanical and thermal loads. The microstructure of AA5050 alloy/ZrC reveals the fracture of interphase and particle. As the volume fraction increases, the particle fracture is initiated at low temperature of thermal loading*

Keywords: *AA5050, zirconium carbide, spherical nanoparticle, RVE model, finite element analysis, interphase fracture.*

1. INTRODUCTION

Composite materials are known to have excellent stiffness and strength characteristics. Thermo-Mechanical loading leads to the initiation and propagation of widespread microstructural damage, often starting with interphasial failure, followed by fracture of the matrix and/or particles in the particle reinforced metal matrix composites. The problems in finding an accurate description of interphase properties are mainly due to the inhomogeneity of the material, i.e. the high stiffness ratio between particles and matrix. In characterizing interphase conditions, experiments on model composites are often accompanied by numerical analyses, qualitatively describing the results of the experiments. To describe the influence of the interphase, numerical micromechanical simulations are often used as an effective too1 [1, 2]. A lot of research was carried out to assess the interface behavior in particle reinforced metal matrix composites under tensile loading using finite element analysis approach [3-18].

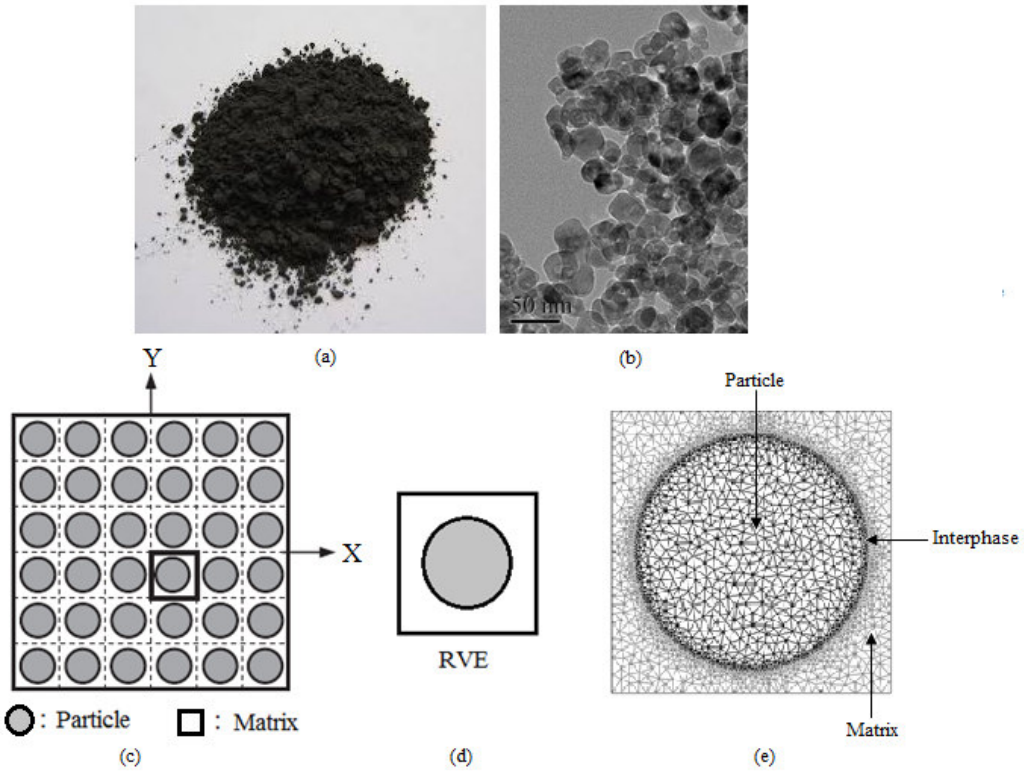

Figure 1: ZrC nanopowder (a) ZrC particles (c) Square array of particles (d) Representative volume element (e) Discretization of RVE.

Zirconium carbide is made by carbo-thermal reduction of zirconia by graphite. Zirconium carbide (ZrC) is an extremely hard refractory ceramic material. The strong covalent Zr-C bond gives this material a very high melting point (~3530 °C), high modulus (~430 GPa) and hardness (25 GPa). Poor oxidation resistance over 800 °C limits the applications of ZrC. One way to improve the oxidation resistance of ZrC is to make composites. In the present work, the effect of thermo-mechanical loading on the fracture in AA5050 alloy/ZrC composites was examined. The shape ZrC nanoparticle considered in this work is spherical. The periodic particle distribution was a square array and corresponding representative volume element (RVE) as shown in figure 1. Both microscopic and micromechanics methods were employed to assess fracture in the composites.

2. MATERIALS METHODS

The matrix material was AA4015 alloy. The reinforcement material was ZrC nanoparticles of average size 100nm. The mechanical properties of materials used in the present work are given in table 1.

Table 1: Mechanical properties of AA5050 matrix and ZrC nanoparticles

Property	AA5050	ZrC
Density, g/cc	2.69	6.73
Elastic modulus, GPa	68.9	430.0
Coefficient of thermal expansion, 10^{-6} 1/°C	21.8	6.8
Specific heat capacity, J/kg/°C	900	368
Thermal conductivity, W/m/°C	193	25
Poisson's ratio	0.33	0.25

(a)

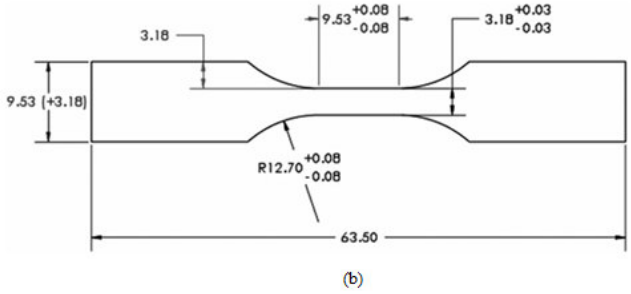

(b)

Figure 2: Tensile testing: UTM with temperature controlled chamber and (b) shape and dimensions of tensile specimen.

AA5050 alloy/ ZrC composites were fabricated by the stir casting process and low pressure casting technique with argon gas at 3.0 bar. The composite samples were give solution treatment and cold rolled to the predefined size of tensile specimens. The heat-treated samples were machined to get flat-rectangular specimens (figure 2) for the tensile tests. The tensile specimens were placed in the grips of a Universal Test Machine (UTM) with temperature controlled chamber at a specified grip separation and pulled until failure. The test speed was 2 mm/min. A strain gauge was used to determine elongation. In the current work, a cubical representative volume element (RVE) was implemented to analyze the tensile behavior AA5050/ZrC nanoparticle composites at two (10% and 30%) volume fractions of ZrC and at different temperatures. The large strain PLANE183 element was used in the matrix in all the models. In order to model the adhesion between the matrix and the particle, a CONTACT 172 element was used.

3. RESULTS AND DISCUSSION

The optical micrograph as shown in figure 4 reveals uniform distribution of ZrC particles in AA5050 alloy matrix.

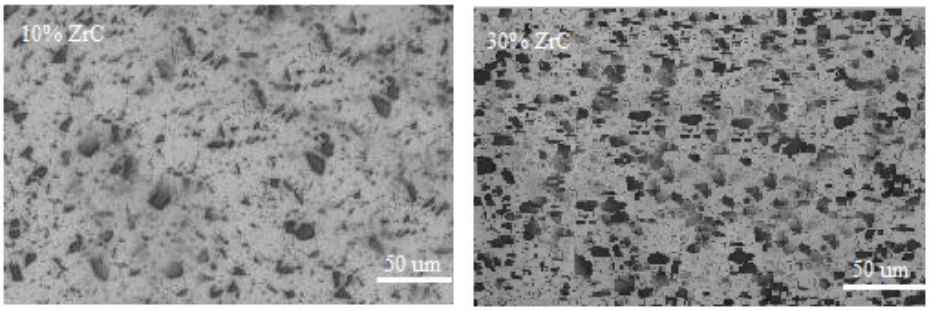

Figure 3: Microstructure showing distribution of ZrC nanoparticles in AA5050 alloy matrix.

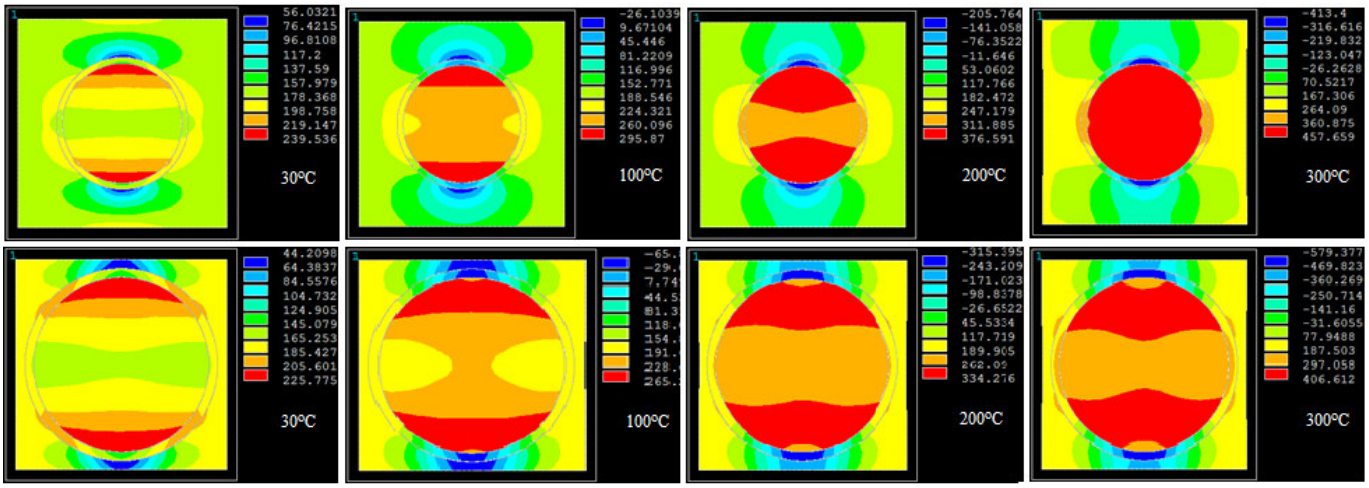

Figure 4: FEA results of tensile stress induced along load direction in the composites comprising of: (a) 10% ZrC and (b) 30% ZrC.

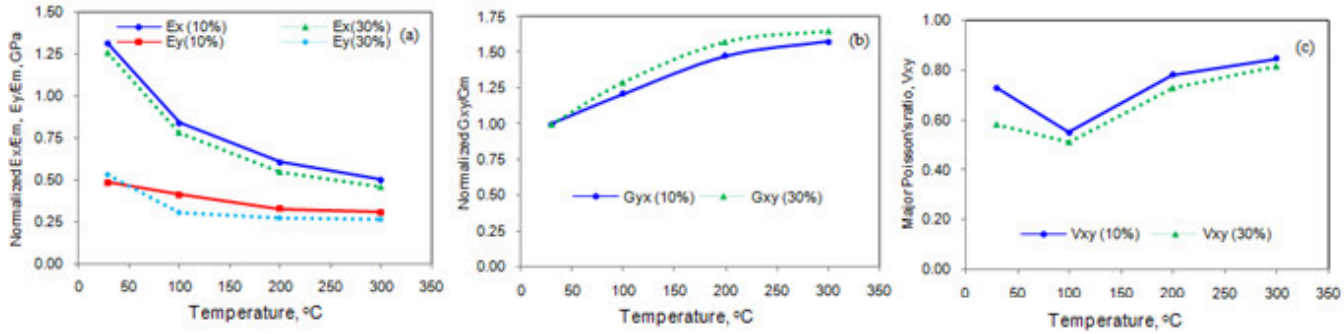

Figure 5: Effect of temperature on micromechanical properties of AA5050/ ZrC composites.

3.1 Thermo-Mechanical Behavior

Figure 4 represents the tensile stresses induced in the AA5050/ZrC composites along the load direction. The tensile stress increases with increase of temperature and it decreases with increase of volume fraction of AA5050/ ZrC in AA5050 alloy matrix. It is observed that the stress induced exceeds the allowable stress as the temperature is increased. The normalized elastic modulus is shown in figure 5a. The elastic modulus is normalized with the elastic modulus of AA5050 alloy. The stiffness of the composites decreases with increase of temperature. The stiffness of AA5050 alloy/10% ZrC composites is higher than that of AA5050 alloy/30% ZrC composites with regard to increase of temperature. The normalized stiffness along the normal direction is lower than that along the load direction. The normalized shear modulus increases with volume fraction of ZrC (figure 5b). Initially, the major Poisson's ratio decrease from 30°C to 100°C and later on it increases with temperature from 100°C to 300°C (figure 5c).

3.2 Fracture Analysis

If the particle deforms in an elastic manner (according to Hooke's law) then,

$$\tau = \frac{n}{2}\sigma_p \quad (1)$$

where σ_p is the particle stress. If particle fracture occurs when the stress in the particle reaches its ultimate tensile strength, $\sigma_{p,uts}$, then setting the boundary condition at

$$\sigma_p = \sigma_{p,\,uts} \quad (2)$$

The relationship between the strength of the particle and the interfacial shear stress is such that if

$$\sigma_{P,uts} < \frac{2\tau}{n} \quad (3)$$

Then the particle will fracture. From the figure 6b, it is observed that the ZrC nanoparticle was not fractured as the condition in Eq. (3) is not satisfied below 200°C for the composites AA5050/10% ZrC composites and below 100°C for the composites AA5050/30% ZrC, respectively. The particle fracture arises above 200°C for the composites AA5050/10% ZrC composites and above 100°C for the composites AA5050/30% ZrC, respectively. This is due to CTE and stiffness mismatches between ZrC nanoparticles and AA5050 alloy matrix. For the interfacial debonding/yielding to occur, the interfacial shear stress reaches its shear strength:

$$\tau = \tau_{max} \quad (4)$$

For particle/matrix interfacial debonding can occur if the following condition is satisfied:

$$\tau_{max} < \frac{n\sigma_p}{2} \quad (5)$$

It is observed from figure 67a that the interphase debonding occurs between ZrC nanoparticle and AA5050 alloy matrix as the condition in Eq.(5) is satisfied below 200°C for the composites AA5050/10% ZrC composites and below 100°C for the composites AA5050/30% ZrC, respectively. The debonding phenomenon is high in the composites comprising of 30% ZrC.

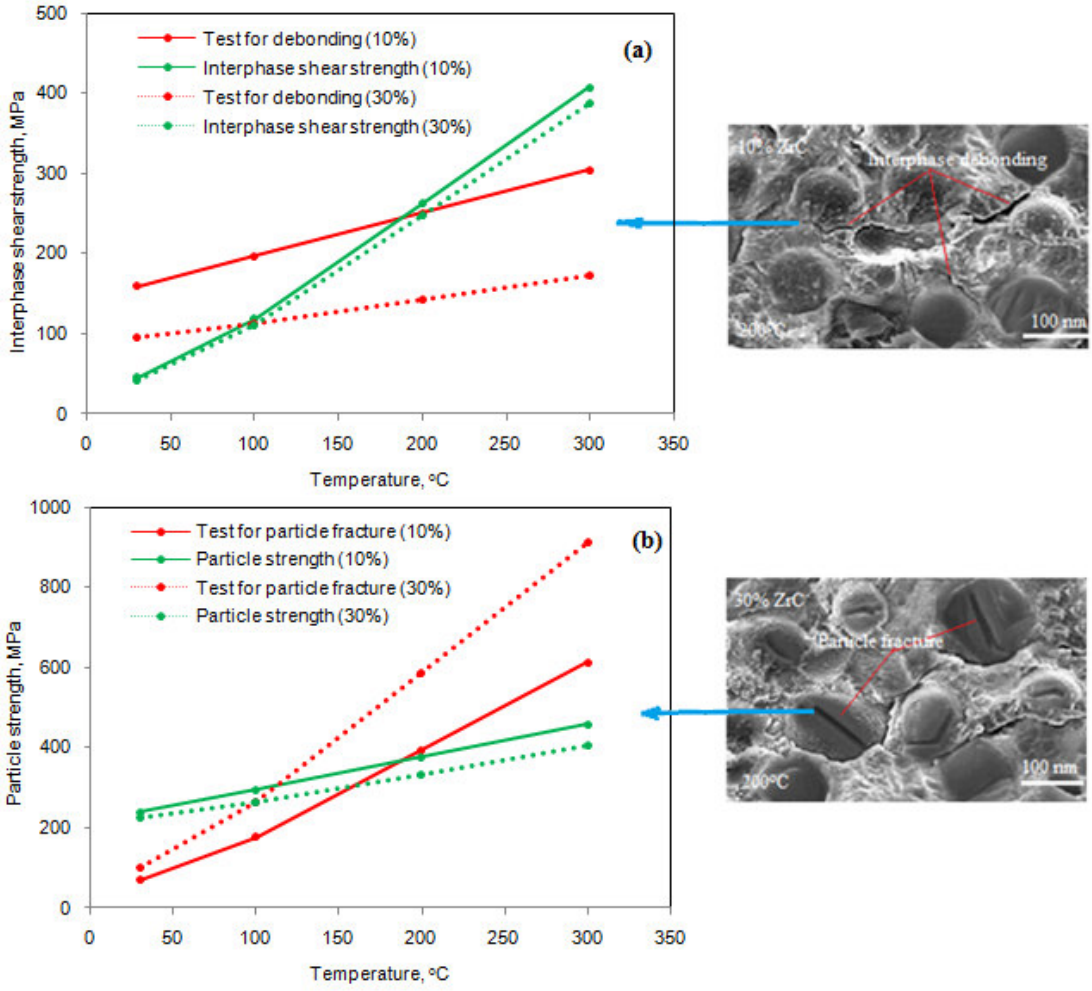

Figure 6: Criterion for interfacial debonding (a) and for particle fracture (b).

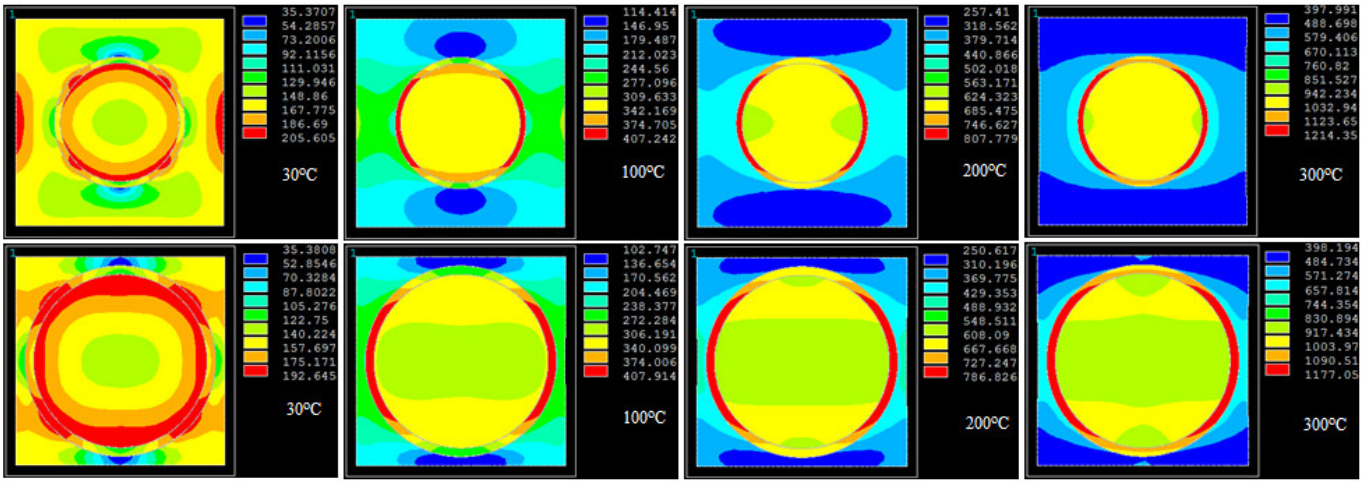

Figure 7: Images of von Mises stresses obtained from FEA: (a) AA5050/10% ZrC and (b) AA5050/30% ZrC composites.

The von Mises stress induced at the interface are higher than that induced in the nanoparticle (figure 7). Hence, the interfacial interphase fracture was occurred between the particle and the matrix. The particle fracture is initiated in AA5050/30% ZrC composites at 100^{o}C of thermal loading and in AA5050/ 10% ZrC composites at 200^{o}C of thermal loading, respectively, due to thermal shock. The microstructure shown in figure 6 confirms the occurrence of interphase and particle fractures in the composites. The interphase debonding increases with increase of temperature.

4. CONCLUSION

The microstructure of AA5050 alloy/ ZrC composites reveals the uniform distribution of ZrC nanoparticles in the matrix. The shear stress is high at the interface resulting to interphase debonding in AA5050/ ZrC composites. The particle fracture is also initiated at 100^{o}C at 100^{o}C of thermal loading and at 200^{o}C of thermal loading AA5050/ 10% ZrC composites, respectively. The microstructure obtained from the experimental samples confirms the fracture of interphase between the ZrC particles and AA5050 alloy matrix and particle fracture.

REFERENCES

1. A. Agbossou, J. Pastor, Thermal Stresses and Thermal Expansion Coefficients of n-Layered Fiber-Reinforced Composites, Composite Science & Technology, 57, 1997, pp. 249-260.
2. J. D. Achenbach, H. Zhu, Effect of Interphases on Micro and Macromechanical Behavior of Hexagonal-Array Fiber Composites, ASME Journal of Applied Mechanics, 57, 1990, pp. 956–963.
3. A. Chennakesava Reddy, Effect of Particle Loading on Microealstic Behavior and interfacial Tractions of Boron Carbide/AA4015 Alloy Metal Matrix Composites, 1st International Conference on Composite Materials and Characterization, Bangalore, March 1997, pp. 176-179.
4. A. Chennakesava Reddy, Reckoning of Micro-stresses and interfacial Tractions in Titanium Boride/AA2024 Alloy Metal Matrix Composites, 1st International Conference on Composite Materials and Characterization, Bangalore, March 1997, pp. 195-197.
5. A. Chennakesava Reddy, Evaluation of Debonding and Dislocation Occurrences in Rhombus Silicon Nitride Particulate/AA4015 Alloy Metal Matrix Composites, 1st National Conference on Modern Materials and Manufacturing, Pune, India, 19-20 December 1997, pp. 278-282,.
6. A. Chennakesava Reddy, Interfacial Debonding Analysis in Terms of Interfacial Tractions for Titanium Boride/AA3003 Alloy Metal Matrix Composites, 1st National Conference on Modern Materials and Manufacturing , Pune, 19-20 December, 1997.
7. A. Chennakesava Reddy, Assessment of Debonding and Particulate Fracture Occurrences in Circular Silicon Nitride Particulate/AA5050 Alloy Metal Matrix Composites , National Conference on Materials and Manufacturing Processes, Hyderabad, India, 27-28 February 1998, pp. 104-109.
8. A. Chennakesava Reddy, Local Stress Differential for Particulate Fracture in AA2024/Titanium Carbide Nanoparticulate Metal Matrix Composites, National Conference on Materials and Manufacturing Processes, Hyderabad, India, 27-28 February 1998, pp. 127-131.

9. A. Chennakesava Reddy, Micromechanical Modelling of Interfacial Debonding in AA1100/Graphite Nanoparticulate Reinforced Metal Matrix Composites, 2nd International Conference on Composite Materials and Characterization, Nagpur, India, 9-10 April 1999, pp. 249-253.
10. A. Chennakesava Reddy, Cohesive Zone Finite Element Analysis to Envisage Interface Debonding in AA7020/Titanium Oxide Nanoparticulate Metal Matrix Composites, 2nd International Conference on Composite Materials and Characterization, Nagpur, India, 9-10 April 1999, pp. 204-209.
11. B. Kotiveera Chari, A. Chennakesava Reddy, Debonding Microprocess and interfacial strength in ZrC Nanoparticle-Filled AA1100 Alloy Matrix Composites using RVE approach, 2nd National Conference on Materials and Manufacturing Processes, Hyderabad, India, 10-11 March 2000, pp. 104-109.
12. A. Chennakesava Reddy, Micromechanical and fracture behaviors of Ellipsoidal Graphite Reinforced AA2024 Alloy Matrix Composites, 2nd National Conference on Materials and Manufacturing Processes, Hyderabad, India, 10-11 March 2000, pp. 96-103.
13. S. Sundara Rajan, A. Chennakesava Reddy, Micromechanical Modeling of Interfacial Debonding in Silicon Dioxide/AA3003 Alloy Particle-Reinforced Metal Matrix Composites, 2nd National Conference on Materials and Manufacturing Processes, Hyderabad, India, 10-11 March 2000, pp. 110-115.
14. S. Sundara Rajan, A. Chennakesava Reddy, Role of Volume Fraction of Reinforcement on Interfacial Debonding and Matrix Fracture in Titanium Carbide/AA4015 Alloy Particle-Reinforced Metal Matrix Composites, 2nd National Conference on Materials and Manufacturing Processes, Hyderabad, India, 10-11 March 2000, 116-120.
15. A. Chennakesava Reddy, Constitutive Behavior of AA5050/MgO Metal Matrix Composites with Interface Debonding: the Finite Element Method for Uniaxial Tension, 2nd National Conference on Materials and Manufacturing Processes, Hyderabad, India, 10-11 March 2000, pp. 121-127.
16. B. Kotiveera Chari, A. Chennakesava Reddy, Interfacial Debonding of Boron Nitride Nanoparticle Reinforced 6061 Aluminum Alloy Matrix Composites, 2nd National Conference on Materials and Manufacturing Processes, Hyderabad, India, 10-11 March 2000, pp. 128-133.
17. P. M. Jebaraj, A. Chennakesava Reddy, Simulation and Microstructural Characterization of Zirconia/AA7020 Alloy Particle-Reinforced Metal Matrix Composites, 2nd National Conference on Materials and Manufacturing Processes, Hyderabad, India, 10-11 March 2000, pp. 134-140.
18. P. M. Jebaraj, A. Chennakesava Reddy, Continuum Micromechanical modeling for Interfacial Debonding of TiN/AA8090 Alloy Particulate Composites, 2nd National Conference on Materials and Manufacturing Processes, Hyderabad, India, 10-11 March 2000, pp. 141-145.